Effect of Repulsive Permanent Magnets on a Cantilever Beam-based Piezoelectric Energy Harvester

Fahmidul Huq Syed
Faculty of Engineering and Technology
Multimedia University
Melaka, Malaysia
famisyed@yahoo.com

Li Wah Thong
Faculty of Engineering and Technology
Multimedia University
Melaka, Malaysia
lwthong@mmu.edu.my

Yee Kit Chan
Faculty of Engineering and Technology
Multimedia University
Melaka, Malaysia
ykchan@mmu.edu.my

2024 Multimedia University Engineering Conference (MECON) | 979-8-3315-3074-7/24/$31.00 ©2024 IEEE | DOI: 10.1109/MECON62796.2024.10776350

***Abstract*— The use of Piezoelectric Energy Harvesters (PEHs) offers a promising solution for emerging low-power electronics and IoT devices. This study investigates the performance of a nonlinear PEH model, which incorporates two permanent magnets in a bimorph configuration. Both analytical methods and COMSOL Multiphysics simulations are employed. The results reveal two distinct peaks, with the maximum voltage and power output reaching 7.83 V and 2.47 mW, respectively, at 74 Hz. It is observed that increasing the distance between the magnets decreases the output results. Although the voltage output closely matches experimental findings, there are slight differences in parameters. A comparison highlights the potential of the nonlinear model to improve output while also acknowledging its inherent complexity. Future research directions include optimizing magnet configurations, integrating with energy management systems, and exploring advanced materials.**

Keywords*— *Energy harvester, Magnets, Nonlinear, Piezoelectricity.

I. INTRODUCTION

In the past decade, the world has unified not only to bring the best of technology but also to create a sustainable earth. When sustainability is discussed, the most common and major factor is renewable energy and its source to satisfy the needs of the growing need of energy in each sector of our work and personal life.

With the rapid growth of industries all across the globe, the growth of wireless technology and microelectronics has been vividly evident. While energy sources like solar and wind holds the possibility of satisfying the energy needs of large infrastructures and machineries, vibration possess a great potential in being the umbrella source for microelectronics, wireless technology and network as well as IoT [1].

Piezoelectric energy harvesting (PEH) methods stands out among the four explored methods of vibration energy harvesting for multiple reasons. The first being its dual effect of converting mechanical stress to electrical output and electrical input to mechanical output, famously known as the direct and reverse piezoelectric effect [2]. However, there are more reasons for preferring PEH over other methods. Its precision based output [3], simple structure and the highest energy density puts it in the center of attention for various devices and applications over the years [4].

The method successfully has been commercialized in various industries over the years. From devices as simple as a lighter to as complex as an atomic clock, the piezoelectric effect is of tremendous use. Implementation of PEH in devices like pacemakers [5], blood pressure monitoring [6] and even tissue engineering [7] is revolutionary in the medical field. Since mid-90's, the US military has implemented PEH for sonic use [8], leading the expand the use of PEH for low powered devices, harnessing energy from the physical movements of the soldiers [9].

The abundance of vibration in nature makes PEH a viable source to be implemented to power IoT devices located in rural or hard to access areas. PEH emergence not only would eliminate the use of batteries but also would subtract the human labor factor to change these batteries from time to time [10].

II. PIEZOELECTRIC ENERGY HARVESTING METHODS

A. Linear Method

Linear piezoelectric energy harvesting method is the conventional technique since it offers a very simple configuration and design with a predictable output [11]. The defining parameters of the mechanical to electrical conversion exhibits a linear relationship causing the optimization of the design simple and easy. The efficient conversion of energy allows the method compatible to linear systems.

However, it truly does not address to the elephant in the room: the bandwidth issue of piezoelectric energy harvesting method [12]. Moreover, the rapid growth of microelectronic devices limits the linear method to attend the power needs [13].

The linear configuration of a transducer is often found in four shapes [13]. The classic configuration is a cantilever beam with a fixed end, having a tip mass atop the open end. The beam set up are famously of two types, a three-layered beam famously known as a bimorph beam where a layer of substrate material is sandwiched between two piezoelectric layers. And a two layered model known as unimorph beam with even distribution of a piezoelectric and substrate layer [11].

Followed by circular diaphragm where the piezoelectric material lays in between a metal shim and electrode. A tip mass situates in the centre to optimise the harvesting capability at lower frequencies [14].

The third design is called cymbal transducer. It is a structure that is built to be efficient at higher impact forces. The shape of the structure allows it to have higher piezoelectric coefficient henceforth leading to higher output generation[15].

Lastly, stack piezoelectric transducer is designed with multiple layers of piezoelectric materials to serve the demand of generating power under higher pressure [14].

B. Nonlinear Method

The linear method is limited to an unsatisfactory bandwidth frequency, the nonlinear method remarkably possesses the capability of attending the bandwidth limitation [16]. However, it exhibits its own shortcomings too. With the capability of harnessing energy at a broader range of frequency with higher energy density, emerges the issue of a complex structure and mechanism [11]. The nonlinearity introduces instability due to the limited understanding of this emerging area.

Nevertheless, the scope of optimizing the range of harnessing energy from PEH method through linear models are more compared to the possible channels through linear model. Nonlinearity in the system could be induced by mechanical stress or stretching [15], mechanical stopper [17], magnetic stopper [18] and magnetic force [19]. Moreover, bi-stable [20], tri-stable and even quad-stable mechanisms allow complex nonlinearity leading to optimized outputs that could potentially serve the growing demand of various microelectronic devices [11].

Adding on to the uncertainties possessed by the complexity and precisive modelling of optimizing techniques, nearby electromagnetic components play a vital role in such system associated with repulsive magnets. External mediums such as amplitude and frequency of vibration leads to highly varying outputs from such systems. Therefore, the outputs achieved from nonlinear piezoelectric energy harvesters are not as predictable as linear piezoelectric energy harvesters.

In the midst of these complex mechanism, there exists relatively simple mechanisms. This paper discusses the implication of a magnetic repulsion induced bi-stable mechanism in depth by showcasing the outcome achieved through a simulation study.

III. METHODOLOGY

A. Theoretical Method

The excitation force on a cantilever-based piezoelectric energy harvester is typically induced by the body load of the mass atop it. This excitation force can be expressed as shown in Equation 1 [21],

$$F_{ex} = \rho_s . g . acc \quad (1)$$

In the context of the first equation, F_{ex} denotes the excitation force, followed by ρ_s , g and acc signifying the density, gravitational constant and base acceleration. In a linear system, this body load is the single source to cause mechanical stress or displacement. However, since in this system nonlinearity is introduced by exchanging the tip mass with a permanent magnet and positioning another permanent magnet at a specific distance with same poles facing one another to induce magnetic repulsion. Therefore, a repulsive force F_r contributes to the force acting in the system and can be expressed as in Equation 2 [22],

$$F_r = \mu x(t) + \lambda x^3(t) \quad (2)$$

Where $\mu x(t)$ defines the linear components and $\lambda x^3(t)$ represents the nonlinear components. The term μ addresses the linear stiffness coefficient and λ signifies the cubic stiffness coefficient, $x(t)$ and $x^3(t)$ represents the displacement and cubic displacement respectively. Addressing the input of both the forces acting in the system, the equation of a repulsive bi-stable piezoelectric energy harvester can be represented in Equation 3 by using Euler-Bernoulli's equation of motion, where M represents the total mass, and C denotes damping, K and θ describe the effective stiffness and equivalent linear piezoelectric electromechanical coupling coefficient [22].

$$M\ddot{x}(t) + C\dot{x}(t) + Kx(t) - \theta v(t) = F(t) + F_r \quad (3)$$

Sine the insertion of magnets creates a nonlinearity that possesses an impulsive excitation, the average power P_{avg} can be calculated using the following equation [13],

$$P_{avg} = \frac{1}{T_{pulse}} \int_{t_1}^{t_2} \frac{V(t)^2}{R} dt = \frac{1}{T_{pulse}} \int_{t_1}^{t_2} I(t)^2 R dt \quad (4)$$

B. Simulation Model

A model was constructed and simulated using COMSOL Multiphysics. The model was constructed in a frequency domain study, further expanding the physics to Solid mechanics, electrostatics, electrical circuits. To introduce piezoelectricity, piezoelectric effect was chosen in the "Multiphysics" option. In order to insert magnets to induce the nonlinearity of the system, magnetic field was added from the "Physics" option.

In the selected domain, firstly the parameters were defined by the user. The resistance, acceleration and the distance between the two permanent magnets were keyed in as displayed in table I.

TABLE I. PARAMETERS

Parameters	Details
Acceleration (acc)	1 ms^{-2}
Resistance (R)	12.5 kΩ
Distance between magnets (d)	2 mm, 4 mm, 6 mm
Frequency range	0-1500 Hz

Upon setting the primary parameters of the study, a two-dimensional geometry of the system was constructed. The geometrical parameters were set in accordance with previously simulated linear FEM models by Malkin et al. [23], followed Syed et al. [24] to verify the legitimacy of the constructed simulation model. The geometric parameters were as follows in Figure 1,

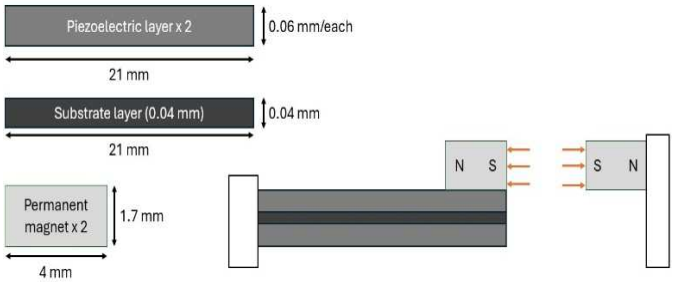

Fig. 1. Geometrical Parameters

The poles of the magnets were defined by the user to enable the repulsion between the two magnets. The beam was constructed with two layers of piezoelectric layer known as a bimorph beam setup to benefit from the extra layer of piezoelectric material. Upon setting the geometrical parameters, materials of each part of the system were defined. The internal material library of COMSOL Multiphysics allowed to define materials from within the system. The mechanical properties of the materials were preexisting in the system, however, the software also allowed user defined properties and materials. The essential mechanical properties of the materials were mentioned alongside the materials in table II.

TABLE II. PROPERTIES OF USED MATERIALS

Material	Young's Modulus (GPa)	Density (kg/m^3)	Poisson's ration
Lead Zirconate Titanate-5A (PZT-5A)	66	7750	0.31
Aluminium (Al)	70	2700	0.33
Neodymium Iron Boron (NdFeB)	160	7500	0.30

Lead Zirconate Titanate-5A (PZT-5A), is an inorganic piezoelectric material which exhibits superior outcomes compared to any organic piezoelectric material such as Polyvinylidene Fluoride Polymer (PVDF). Hence, it was used instead of PVDF although PVDF is a widely used piezoelectric material due to its cost effectiveness and availability. Aluminium was used for the substrate layer due to its showcasing of a broader frequency bandwidth in a study performed by Syed et al. [24]. Neodymium iron boron (NdFeB) was used as a material for permanent magnets. Once the materials were successfully defined, a proper "Meshing" of the model was done. Next the model was simulated in a range of 0-1500 Hz. For a linear system, the investigated range of frequency is shorter than a nonlinear model since a nonlinear model possesses the capability of harnessing energy from a wider range of frequencies. The obtained data from the simulation is revealed and discussed in the following section.

IV. RESULTS AND DISCUSSION

The nexus between bi-stable magnets and the existing distance in between them is theoretically dominated by the margin of distance. With growing distance, the repulsive force weakens. Abiding by the parameters mentioned in Tables I and II, a 2D model of the piezoelectric cantilever beam was modelled in COMSOL Multiphysics. The varying parameters were changed accordingly in the system to attain results.

A. Validation of the Model

The current model was first compared as a linear model prior to introducing nonlinearity in the system with a linear FEM study conducted by Malkin et al [23]. Similarly, it was compared to the linear model of Syed et al. [24][25]. Once nonlinearity was exposed to the system, the model was compared to a mono stable magnetic FEM study conducted by Jaafar et al. [21]. Moreover, the data was compared to a similar experimental study performed by Thong et al. [22]. The current model exhibits similar results as a linear system and as a nonlinear system to the respective comparative studies. A comparative chart would be showcased at the end of the section versus the similar respective studies highlighting the differences resulting to some minor differences in results.

B. Stress Distribution

The stress distribution of the model plays a vital role in energy conversion due to the direct impact of bending stress in voltage generation. The relationship between stress and voltage generation could be expressed as follows,

$$V = \sigma + g_{3j} + L \tag{5}$$

In the context of the equation mentioned above, σ denotes the stress, g_{3j} is the piezoelectric constant and L is the length of the beam. The effect of the length has already been proved in a study lead by Tong et al. [26]. In the current study, the stress distribution of the model was as displayed in Figure 2. The stress acting on the beam surface was quite low as it can be seen on the impact scale on the right corner of Figure 2. This is due to the low acceleration of the model as defined in the parameters. Increase of the acceleration would rapidly increase the force of excitation generated by the body load as defined in Equation 1, leading to a higher output generation of the system.

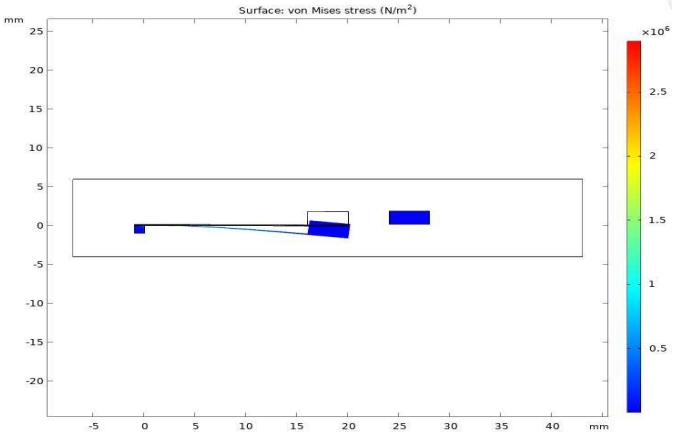

Fig. 2. Stress Distribution

C. Voltage and Power Responses

In a nonlinear system, the voltage and power generation showcases some uncertainty, hence it causes difficulties in predicting an exact or close estimation of power generation compared to a linear model. The data acquisition of the model

was done by performing three simulation computation by varying the distance between the two magnets. Each computation generated a voltage and electrical power output in a frequency domain. The voltage graph for each distance were merged for comparison as displayed in Figure 3,

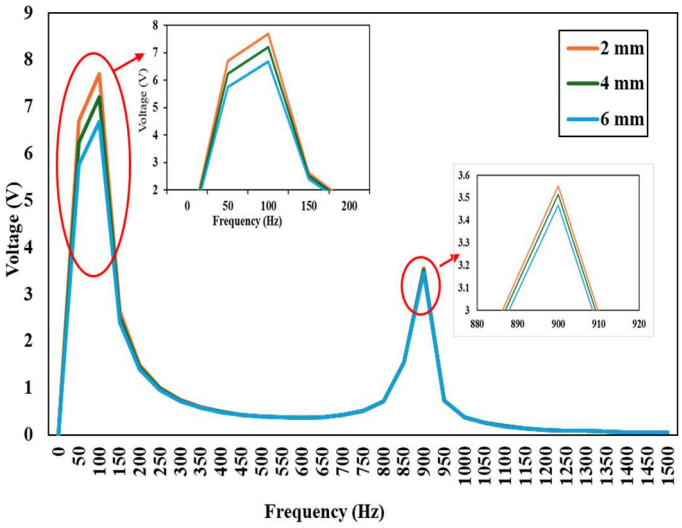

Fig. 3. Voltage Output

Theory concludes that with emerging distance, the force between two magnets weakens [22]. The obtained data presented in Figure 3 justifies the theory. As the distance is increase, a decrease in voltage is noticed, especially on the first peak. However, the resonance frequency of all three distances appeared to be same. This is due to the fact that only the magnet placed on top of the beam works as the proof mass that effects the resonant frequency. The graph displayed two peaks at two different frequencies. The second rise of voltage leading two the second peak displayed 3.55 V, 3.51 V and 3.44 V at 2 mm, 4 mm and 6 mm distance respectively at 900 Hz. The magnitudes of the harmonic peaks very significantly higher than any occurrence of a harmonic peak in a linear model, which was observed on a substrate material-based study performed by Syed et al. [24]. A clear difference in the magnitude of the voltage output was noticed in the first peak. The highest peak was noticed when the magnets were 2 mm apart, with a voltage output of 7.83 V at at 100 Hz. Once the two magnets were positioned at 4mm and 6mm apart from one another, the voltage decreased as they generated 7.2 V and 6.9 V respectively. This is due to the decrease in the repulsive force between the two magnets as mentioned in Equation 2.

Similar to the voltage graph, the electrical power graph displayed similar trajectory in its output as shown in Figure 4. The first peak emerged at 100 Hz and the second emerged at 900 Hz. The highest peak generated 2.47 mW with the closest distance between the magnets. Electrical outputs of 2.32 mW and 2.23 mW were produced once the magnets were repositioned 4 mm and 6 mm away from one another.

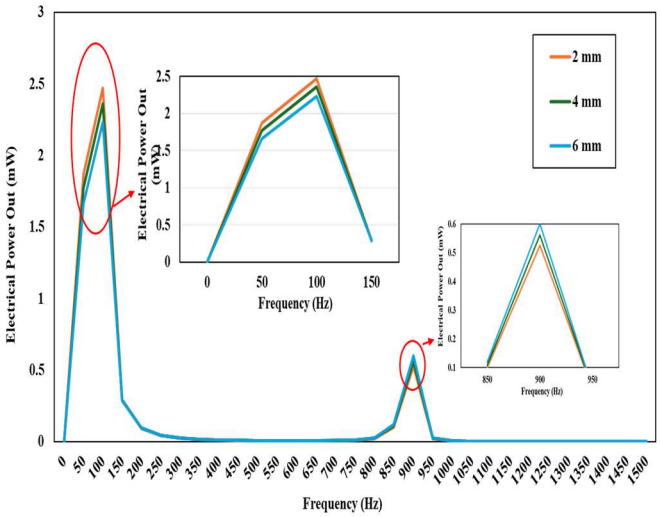

Fig. 4. Electrical Power Output

Since the simulation covered a very wide bandwidth of 0-1500 Hz, therefore, the iterations were minimized by simulating with an iteration jump of 50 Hz. Once the data were achieved, to observe a smoother curve of the outputs, the simulation was re conducted within the range of resonance as shown in Figures 5 and 6, displaying the voltage and electrical power output of the first peak.

These two Figures identify the exact resonance frequency due to simulating the model covering each frequency. The first peak occurred at 74 Hz and the second peak rose at 886 Hz.

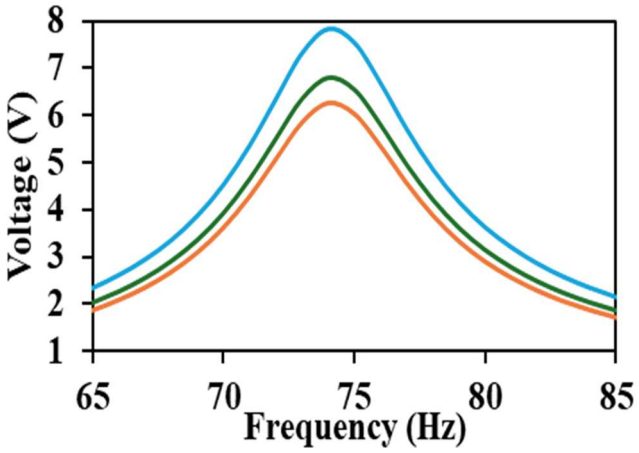

Fig. 5. Voltage Graph at Resonance Bandwidth

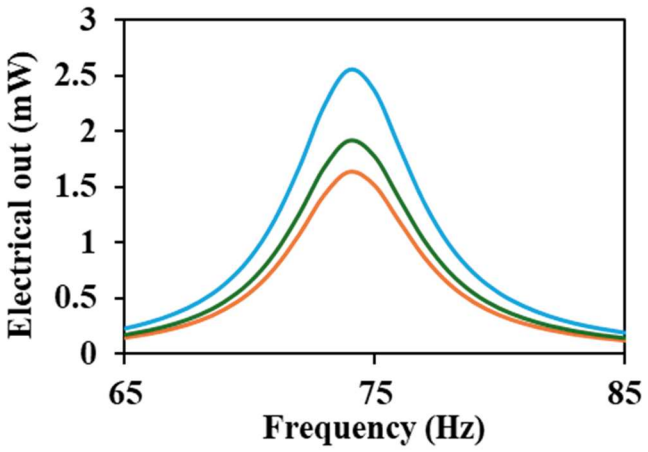

Fig. 6. Electrical Power Graph at Resonance Bandwidth

D. Comparison

The comparison of the current nonlinear model was drawn against a mono stable FEM model studied by Jafaar et al. [21]. Moreover, an additional comparison was done against the experimental study administered by Thong et al. [22]. Since there are unpredictable factors effecting nonlinearity, hence, it is difficult to generate mirroring outcome. However, the objectives of these studies allow a window to compare them under one scale.

Figure 7 displayed a comparison of the voltage outcome generated by each models as mentioned above. The experimental model generated almost identical results at similar parameters, where the magnets were situated with a gap of 2mm between. The reason the mono stable model displayed lower magnitude of outcome is due to the fact that only the body load is acting as a force on the beam, whilst in the current and experimental model, there is an addition of repulsive force that contributes to the achievement of a higher output.

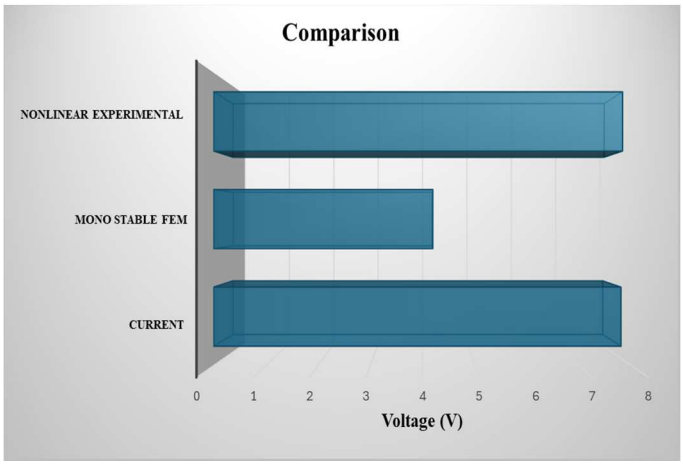

Fig. 7. Comparison of Current Model

V. Conclusion

This study builds a bridge supporting the theory of the effect of distance between two magnets effecting the outcome of a piezoelectric energy harvester's output generation through evident data. This study also establishes the potential of harvestable energy at higher frequency ranges. It has been an area of interest to build better sonic devices since piezoelectric method is an existing method in the military. The nonlinear model generated high magnitudes of voltage and electrical power that supports experimental data which has been explored in the past. However, since this study was performed using geometrical parameters which were millimetre-sized, improving the size for experimental use would possess potential of generating higher conversion of mechanical stress to electrical output. Moreover, the study's focus on a specific frequency range (0-1500 Hz) may not capture the full range of frequencies in which the system can operate.

Acknowledgment

This work was supported by the Ministry of Higher Education of Malaysia under the Fundamental Research Grant Scheme (FRGS/1/2020/TK0/MMU/03/13). The authors would also like to acknowledge the Faculty of Engineering and Technology, Multimedia University for the support given in conducting this research.

References

[1] K. Aouali, N. Kacem, N. Bouhaddi, and M. Haddar, "On the optimization of a multimodal electromagnetic vibration energy harvester using mode localization and nonlinear dynamics," *Actuators*, vol. 10, no. 2, pp. 1–19, 2021, doi: 10.3390/act10020025.

[2] Y. Chen, B. W. Lu, D. P. Ou, and X. Feng, "Mechanics of flexible and stretchable piezoelectrics for energy harvesting," *Sci. China Physics, Mech. Astron.*, vol. 58, no. 9, 2015, doi: 10.1007/s11433-015-5692-5.

[3] S. F. Nabavi, A. Farshidianfar, A. Afsharfard, and H. H. Khodaparast, "An ocean wave-based piezoelectric energy harvesting system using breaking wave force," *Int. J. Mech. Sci.*, vol. 151, pp. 498–507, 2019, doi: 10.1016/j.ijmecsci.2018.12.008.

[4] M. S. Woo *et al.*, "Study on increasing output current of piezoelectric energy harvester by fabrication of multilayer thick film," *Sensors Actuators, A Phys.*, vol. 269, pp. 524–534, 2018, doi: 10.1016/j.sna.2017.12.025.

[5] K. Meng *et al.*, "Flexible Weaving Constructed Self-Powered Pressure Sensor Enabling Continuous Diagnosis of Cardiovascular Disease and Measurement of Cuffless Blood Pressure," *Adv. Funct. Mater.*, vol. 29, no. 5, pp. 1–10, 2019, doi: 10.1002/adfm.201806388.

[6] L. Y. Chen *et al.*, "Continuous wireless pressure monitoring and mapping with ultra-small passive sensors for health monitoring and critical care," *Nat. Commun.*, vol. 5, pp. 1–10, 2014, doi: 10.1038/ncomms6028.

[7] J. Liu, H. Gu, Q. Liu, L. Ren, and G. Li, "An intelligent material for tissue reconstruction: The piezoelectric property of polycaprolactone/barium titanate composites," *Mater. Lett.*, vol. 236, pp. 686–689, 2019, doi: 10.1016/j.matlet.2018.11.036.

[8] W. S. Hwang *et al.*, "Design of piezoelectric ocean-wave energy harvester using sway movement," *Sensors Actuators, A Phys.*, vol. 260, pp. 191–197, 2017, doi: 10.1016/j.sna.2017.04.026.

[9] I. Izadgoshasb, Y. Y. Lim, N. Lake, L. Tang, R. V. Padilla, and T. Kashiwao, "Optimizing orientation of piezoelectric cantilever beam for harvesting energy from human walking," *Energy Convers. Manag.*, vol. 161, no. December 2017, pp. 66–73, 2018, doi: 10.1016/j.enconman.2018.01.076.

[10] R. Esmaeeli *et al.*, "A Rainbow Piezoelectric Energy Harvesting System for Intelligent Tire Monitoring Applications," *J. Energy Resour. Technol.*, vol. 141, no. 6, Jan. 2019, doi: 10.1115/1.4042398.

[11] H. Liu, J. Zhong, C. Lee, S. W. Lee, and L. Lin, "A comprehensive review on piezoelectric energy harvesting technology: Materials, mechanisms, and applications," *Appl. Phys. Rev.*, vol. 5, no. 4, 2018, doi: 10.1063/1.5074184.

[12] L. Tang and J. Wang, "Size effect of tip mass on performance of cantilevered piezoelectric energy harvester with a dynamic

magnifier," *Acta Mech.*, vol. 228, no. 11, pp. 3997–4015, 2017, doi: 10.1007/s00707-017-1910-8.

[13] C. Covaci and A. Gontean, "Piezoelectric energy harvesting solutions: A review," *Sensors (Switzerland)*, vol. 20, no. 12, pp. 1–37, 2020, doi: 10.3390/s20123512.

[14] N. S. Shenck and J. A. Paradiso, "Energy scavenging with shoe-mounted piezoelectrics," *IEEE Micro*, vol. 21, no. 3, pp. 30–42, 2001, doi: 10.1109/40.928763.

[15] H. Li, C. Tian, and Z. D. Deng, "Energy harvesting from low frequency applications using piezoelectric materials," *Appl. Phys. Rev.*, vol. 1, no. 4, 2014, doi: 10.1063/1.4900845.

[16] D. D. Quinn, A. L. Triplett, L. A. Bergman, and A. F. Vakakis, "Comparing Linear and Essentially Nonlinear Vibration-Based Energy Harvesting," *J. Vib. Acoust.*, vol. 133, no. 1, Dec. 2010, doi: 10.1115/1.4002782.

[17] H. Liu, C. Lee, T. Kobayashi, C. J. Tay, and C. Quan, "Investigation of a MEMS piezoelectric energy harvester system with a frequency-widened-bandwidth mechanism introduced by mechanical stoppers," *Smart Mater. Struct.*, vol. 21, no. 3, 2012, doi: 10.1088/0964-1726/21/3/035005.

[18] X. Wang *et al.*, "A frequency and bandwidth tunable piezoelectric vibration energy harvester using multiple nonlinear techniques," *Appl. Energy*, vol. 190, pp. 368–375, 2017, doi: 10.1016/j.apenergy.2016.12.168.

[19] K. Fan *et al.*, "A monostable piezoelectric energy harvester for broadband low-level excitations A monostable piezoelectric energy harvester for broadband low-level excitations," vol. 123901, pp. 5–10, 2018, doi: 10.1063/1.5022599.

[20] A. Erturk, J. Hoffmann, and D. J. Inman, "A piezomagnetoelastic structure for broadband vibration energy harvesting," *Appl. Phys. Lett.*, vol. 94, no. 25, 2009, doi: 10.1063/1.3159815.

[21] M. I. Jaafar, H. M. M. M. Rabah, N. H. D. Nordin, A. G. A. Muthalif, and A. N. Wahid, "Voltage Generation in Piezoelectric Energy Harvesting with Magnet: FEA Simulation and Experimental Analysis," *J. Sci. Technol.*, vol. 13, no. 2, pp. 17–24, 2021, doi: 10.30880/jst.2021.13.02.003.

[22] L. W. Thong, S. L. Kok, and R. Ramlan, "Parameter Optimization of Nonlinear Piezoelectric Energy Harvesting System for IoT Applications," *Int. J. Adv. Comput. Sci. Appl.*, vol. 13, no. 5, pp. 355–363, 2022, doi: 10.14569/IJACSA.2022.0130542.

[23] M. C. Malkin and C. L. Davis, "Multi-frequency piezoelectric energy harvester," *J. Acoust. Soc. Am.*, vol. 118, no. 1, p. 24, 2005, doi: 10.1121/1.1999402.

[24] F. H. Syed, L. W. Thong, and Y. K. Chan, "Evaluation of Substrate Materials and Mass Structure on Piezoelectric Cantilever Based Energy Harvester," *J. Eng. Sci. Technol.*, vol. 18, no. 6, pp. 3140–3154, 2023.

[25] F. H. Syed, L. W. T. B, and Y. K. Chan, *Proceedings of the Multimedia University Engineering Conference (MECON 2022)*. Atlantis Press International BV, 2023.

[26] W. P. Q. Tong, B. M. S. Muhammad Ramadan, and T. Logenthiran, "Design and Simulation of a Piezoelectric Cantilever Beam for Mechanical Vibration Energy Harvesting," *Int. Conf. Innov. Smart Grid Technol. ISGT Asia 2018*, pp. 1245–1250, 2018, doi: 10.1109/ISGT-Asia.2018.8467796.